



Sharif University of Technology
Scientia Iranica
Transactions A: Civil Engineering
www.scientiairanica.com



A parametric study of seismic response in anchored steel tanks with endurance time method

D. Vaezi, H.E. Estekanchi* and A. Vafai

Department of Civil Engineering, Sharif University of Technology, Tehran, Iran.

Received 22 October 2013; received in revised form 20 October 2013; accepted 10 December 2013

KEYWORDS

Seismic assessment;
Anchored steel tanks;
Endurance time
method;
Fluid-structure
interaction;
Cylindrical shells.

Abstract. In this paper, the seismic response of anchored cylindrical steel tanks with various dimensional parameters has been investigated by endurance time method considering fluid-structure interaction effects. Various response quantities, such as stresses and displacements, have been evaluated by subjecting tanks to specially designed intensifying accelerograms and their performance is judged based on their response at predefined level(s) of dynamic excitation. It is shown that ET analysis can reliably predict the result of ground motion time history analysis in all seven tank models studied. In four of the tanks in which height of the shell and the level of fluid is the same, the variation of significant parameters with height to diameter ratio is discussed. The reliability of the ET method in predicting the response of models considering nonlinear material and geometric nonlinearity is also investigated using a limited number of models. In general, results by endurance time method, while entailing highly reduced computational demand, appear to be reasonably consistent with those from ground motions in anchored steel tanks analysis considering fluid-structure interaction.

© 2014 Sharif University of Technology. All rights reserved.

1. Introduction

Assessment of the seismic safety of liquid storage tanks is among challenging problems in earthquake engineering. The existence of fluid and solid shell alongside each other and liquid-structure interaction gives distinctive properties to these structures. Many researchers have studied these structures in the past. Housner (1954) showed that there are two dominant mode shapes in vibration of tanks. The impulsive part includes a solid shell and adjacent liquid that oscillates together; this component has a low period and the other component is the convective or sloshing component that is related to the remaining portion of

the liquid that causes wave and sloshing at the top of tanks and has a long period. Some properties, such as base shear (V) and Overturning Moment (OM), depend on the impulsive component and some of the others, like sloshing and wave height, are related to the convective or sloshing component [1]. Later, Malhotra [2] improved Housner's model, as shown in Figure 1. On ground cylindrical steel storage tanks are one of the most important and versatile tanks. The high capacity of these tanks and the variety of liquids they hold make them appealing to industrial facilities. Collapse of these tanks in addition to direct damage to the structure of tank may cause indirect vulnerability, such as environmental pollution and fire examples of which are evident in recent earthquakes [3]. Therefore, estimation of stability and resistance of liquid storage tanks against earthquakes is important. Time history method is the most precise method of assessing seismic performance of structures. The Endurance Time (ET) method is a dynamic pushover procedure that tries to

*. Corresponding author. Tel.: +98 21 66164212;
Fax: +98 21 66014828
E-mail addresses: dvaezi@yahoo.com (D. Vaezi),
stekanchi@sharif.edu (H.E. Estekanchi), vafai@sharif.edu (A. Vafai)

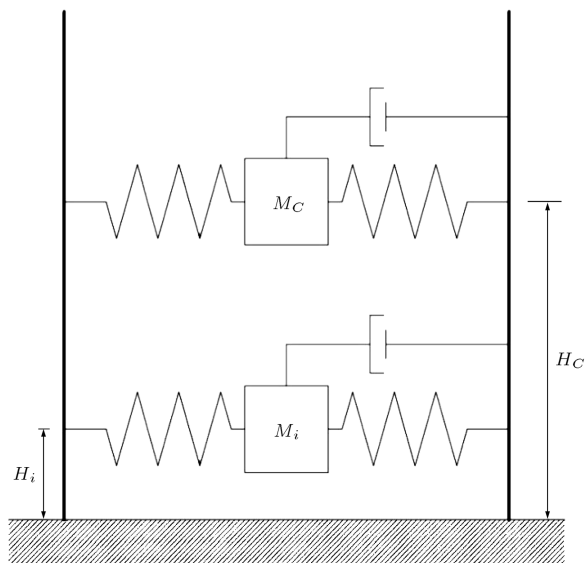


Figure 1. Analytic model of the tank and its content.

predict the engineering demand parameters at different intensity levels by subjecting the structures to some predesigned intensifying dynamic excitations [4]. ET method can be used for seismic analysis and design of various kinds of structures [5,6], and is based on time history analysis. Theoretical feasibility of ET method in linear and nonlinear analysis has been proved [7-10]. In this study, parameters such as the stress and displacement of cylindrical steel tanks with various dimensions are investigated. Performance of ET method in assessing seismic parameters of typical cylindrical steel storage tanks subjected to a series of acceleration functions is investigated in seven tanks of different configurations.

2. Concept of ET method

The main objective in this method is to provide an analysis method based on time history analysis applicable to a wide range of structural systems that do not easily yield themselves to static pushover or modal analysis procedures. The basic concept of ET analysis can be explained by a hypothetical shaking table experiment. It is assumed that three different structures (or design alternatives of the same structure) with unknown structural properties are to be ranked according to their seismic resistance performance. All three structures are fixed on a shaking table and the test begins by subjecting the structures to a very low amplitude random vibration, as shown in Figure 2(a). The experiment starts by gradually increasing the amplitude of the shaking table vibrations. As the vibration amplitude increases, a point will be reached when one of the structures (say structure number '1') fails as shown in Figure 2(b). As the amplitude of vibration further increases, a point will be reached

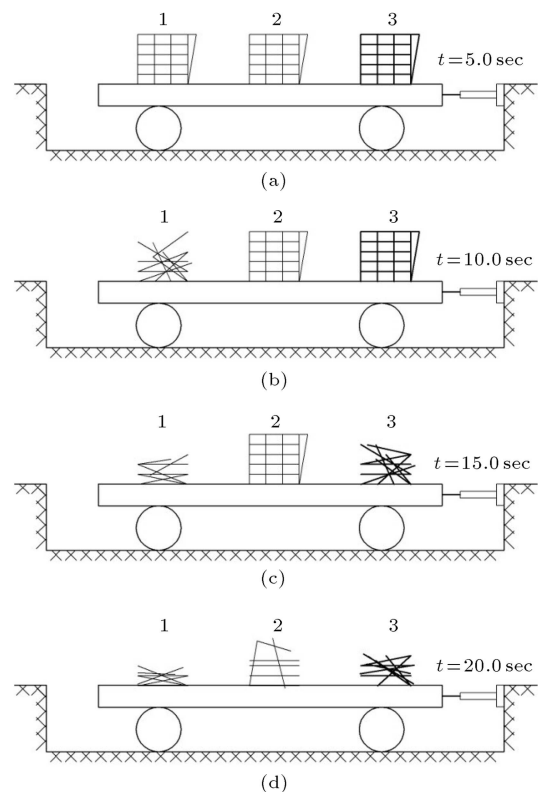


Figure 2. Hypothetical shaking table experiment.

when the second and third structures will also fail. This has been shown in Figure 2(c) and (d) where structure '3' has failed at say, $t = 15$ sec and structure '2' has failed at, say, $t = 20$ sec. Based on these results, and assuming that the lateral loads induced by the shaking table correspond with the earthquake induced excitations, structure '1', which failed earliest, is ranked as the worst performer and structure '2', which endured longer, is ranked as the best performer. This hypothetical experiment describes the essence of endurance time method. In the ET method, structures are subjected to a chosen instrumentally intensifying accelerogram and their performance is studied based on the time interval during which they can meet a predefined set of performance criteria, e.g., resisting failure in the above test. This is somewhat similar to IDA, however, in ET analysis, the entire range of intensity levels is covered in a single response history analysis, thereby considerably reducing the computational demand for a reasonably realistic dynamic analysis.

A computational interpretation of the above test can be developed for practical applications. Considering that the representative finite element structural models of the prototypes used in the test are available, and assuming that an appropriate ET acceleration function has been provided, the above-mentioned test procedure can be numerically replicated. After a representative finite element model has been constructed

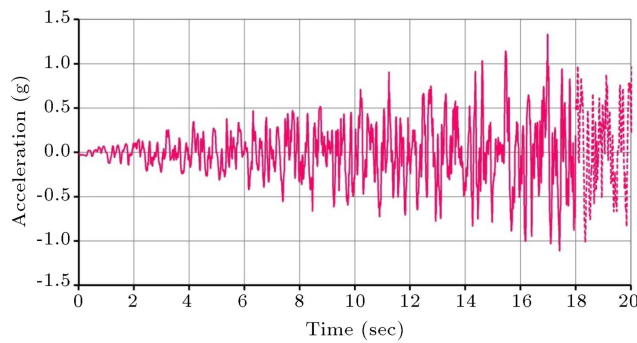


Figure 3. Plot of a typical ET acceleration function (series “ETA20e”).

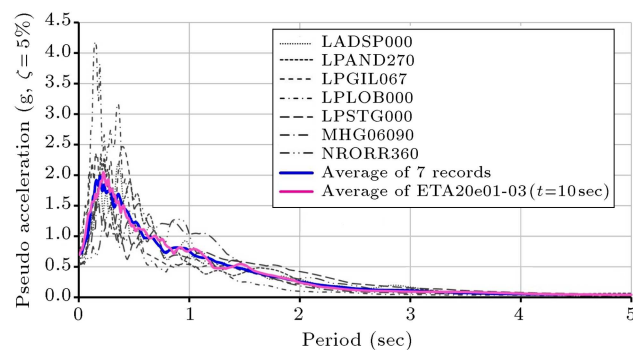


Figure 4. Response spectra of selected records and their average.

and a suitable damage measure (such as stress levels, displacement limits, damage indexes, etc.) is set, ET dynamic analysis can be performed [4]. In this paper, ET acceleration function series “ETA20e” have been used. These acceleration functions are publicly available through internet [11]. The acceleration and displacement response spectrum of these series is consistent with typical ground motions on stiff soil. In fact, average response spectra of 7 ground motions on stiff soil were used in generating these records [4].

A typical plot of an acceleration function of “ETA20e” series is shown in Figure 3. This graph shows the general trend of acceleration intensification with time. A key point in successful estimation of response to ground motions at different intensity levels by the ET method is incorporation of the concept of response spectra in generation of ET acceleration functions.

As can be seen in Figure 3, the envelope of ET excitation is not similar to an earthquake. In fact, this is an infinitely intensifying excitation. However, this excitation has an interesting property that each window of it, from $t = 0$ up to a particular time, produces a response spectrum that corresponds to a target spectrum with a scale factor. In Figure 4, the response spectra of selected ground motions and their average response spectrum are shown. This average

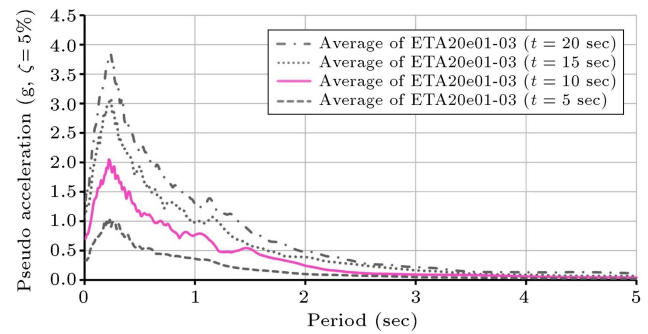


Figure 5. Average acceleration spectra induced by “ETA20e” series at various times.

is used as template spectrum in generating “ETA20e” series of ET acceleration functions. As can be seen here, the average response spectrum of “ETA20e” series conforms to average response spectrum of earthquakes records. Also, as can be seen in Figure 4, by using the average of three acceleration functions, better accuracy in matching the target spectrum can be achieved for this set of accelerograms. This correlation between response spectra of ET and ground motions is a key property that enables good estimation of structural response through intensifying ET acceleration functions as will be explained next.

In Figure 5, it is shown that the response spectrum of an ET acceleration function intensifies proportionally with time. This would imply that at $t = 2t_{\text{Target}}$, the response is theoretically double the target value, at $t = 3t_{\text{Target}}$, it is triple the target value, and at $t = 4t_{\text{Target}}$, it is four times the target value, etc. In this way, the target acceleration response of ET acceleration function is defined, as in Eq. (1):

$$S_{aT} = (T, t) = \frac{t}{t_{\text{Target}}} S_{aC}(T), \quad (1)$$

where $S_{aT}(T, t)$ is the target acceleration response of ET acceleration function at time t , T is the period of free vibration, and $S_{aC}(T)$ is the template acceleration spectra that can be from code or an appropriate response spectra pertaining to site conditions. In this way, the spectrum of ET acceleration functions ideally should remain proportional to template spectrum $S_{aC}(T)$ at all times t . In practice, exact match cannot be achieved, however, as shown in Figure 5., this requirement has been satisfactorily met. It should be noted that almost the same level of conformity has been achieved at all times, rather than the samples taken at 5, 10, 15 and 20 sec shown in Figure 5 [12].

3. Liquid storage tanks models

3.1. Design of tanks

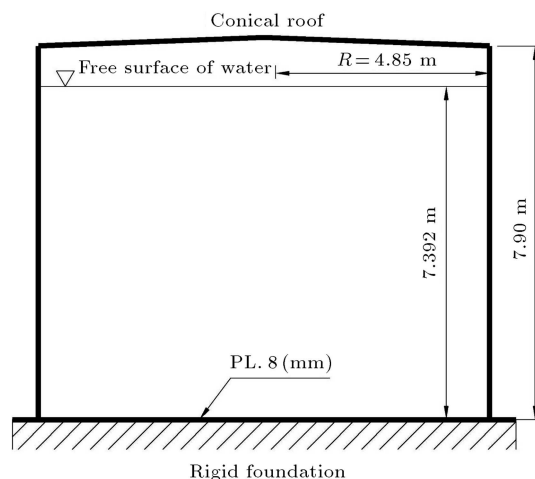
In this study, seven tanks with different geometric dimensions were considered. Six of these tanks have

Table 1. Geometric specifications of tanks.

Name	Ht/D	Ht (m)	H (m)	Hr (m)	R (m)	$t1$ (mm)	$t2$ (mm)	$t3$ (mm)	$t4$ (mm)	$t5$ (mm)	$t6$ (mm)
D48H12	0.25	12	10.5	13.2	24	25	20	15	10	-	-
D32H12	0.375	12	10.5	12.8	16	16	12	8	6	-	-
D16H12	0.75	12	10.5	12.4	8	8	6	6	6	-	-
D08H12	1.50	12	10.5	12.2	4	6	6	6	6	-	-
Tank A	0.81	7.9	7.392	8.023	4.85	8	-	-	-	-	-
D32H18	0.56	18	16.5	18.8	16	25	20	18	15	10	8
D08H06	0.75	6	4.5	6.2	4	6	6	-	-	-	-

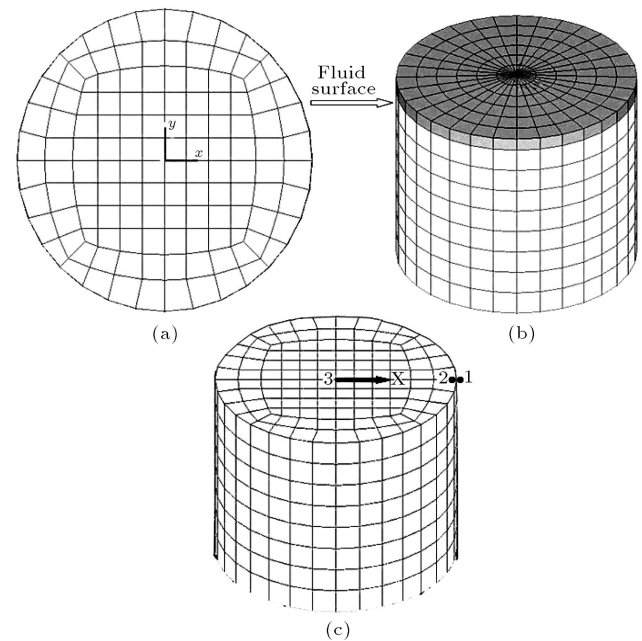
Table 2. Fluid and steel properties.

Design parameters	Quantity
Bulk modulus (GPa)	2.07
Fluid density (kg/cm^3)	1000
Fluid viscosity (Ns/m^2)	0.00113
Steel's module of elasticity (GPa)	204
Steel density (Kg/cm^3)	7800
Poisson's ratio	0.27

**Figure 6.** General properties and dimensions of Tank A.

been designed based on recommendations of API [13] and Chapter 12 of “Iranian seismic design code for oil industries” [14]. The design of one of the tanks has been taken exactly from Barton and Parker [15]. This tank, referred to as “Tank A”, is used for verification of the numerical model. In Figure 6, a section of this tank is shown. In Table 1, the geometric parameters of these tanks are enlisted.

Thickness of Tank A is constant over its height and is equal to 8 mm. The remaining six tanks have variable thickness over height; each strip of shell in height was considered to be 3 meters. These tanks have fixed conical roofs with 1/20 slope, the thickness of the roof plates is 5 mm and the thickness of the bottom plate is 6 mm. In Table 2, the properties

**Figure 7.** Finite element model of a typical tank.

of the fluid and the steel are defined. For nonlinear analysis, yield stress of steel is considered to be 240 MPa, and the stress-strain model is considered to be as a bilinear kinematic with 3% slope on plastic region.

3.2. FE modeling

In this paper, finite element three-dimensional geometric models with solid and fluid elements were considered as shown in Figure 7(b). In order to arrive at a reliable model, a cross section of the tank's cylinder has been considered in drawing a typical meshing of circular plan with well proportioned quadrilateral elements (Figure 7(a)) and then relevant nodes and elements are imported into numerical model. All bottom nodes are assumed to be completely fixed on the base. All periphery nodes of fluid are coupled to relevant nodes of the solid shell in normal direction (Figure 7(c), e.g. nodes 1 and 2). As Figure 7(c) shows, the dynamic movement is applied in one direction (axis x) on the horizontal plane [6,7].

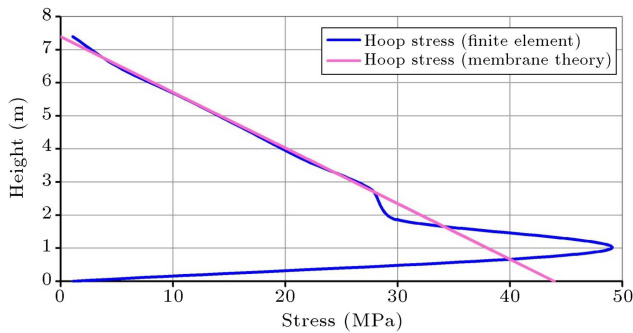


Figure 8. Comparison of hoop stresses in FE and membrane theory.

3.3. Model verification

After considering Tank A, the first static analysis on this model was performed and hydrostatic pressure counters were compared with the theoretical quantity:

$$P = \gamma H. \quad (2)$$

The results of FE were consistent with theoretical values. Response spectrum analysis was then performed on Tank A by using the spectrum as taken exactly from Barton and Parker [15] in order to verify the model. Other various controls, such as mode shapes and periods of vibration, were also checked to insure the acceptable model performance.

4. Results of analyses

4.1. Static analysis

After calculating the hydrostatic pressure, the hoop stress of the shell walls was derived from the model and it was compared against the theoretical value from membrane analysis. The results for “Tank A” are shown in Figure 8. Some discrepancies between FE and theoretical results are due to the fact that in the FE model, the wall is fixed at the bottom eliminating the possibility of hoop stress development. Membrane theory does not apply to the areas near the boundary. As can be seen, the results are compatible at reasonable distances from the boundary. A more accurate state of stresses in the boundary region can be achieved by employing a more refined mesh, requiring higher computational effort. However, the proposed model is believed to be appropriate considering the goal of this research, i.e. a general comparative study requiring extensive response history analyses.

4.2. Modal analysis

Modal analysis is performed on all tanks in order to acquire the dynamic parameters of tanks that are used for verification of models with analytic results and for calculation of the damping matrix that will be used in time history analyses. Dynamic parameters of tanks are shown in Table 3, where f_1 , m_1 , f_{01}

Table 3. Dynamic parameters of tanks.

Name	H/D	f_1 (Hz)	m_1 (%)	f_{01} (Hz)	m_{01} (%)
D48H12	0.25	0.11	59	4.64	24
D32H12	0.37	0.15	49	5.15	34
D16H12	0.75	0.23	29	6.42	51
D8H12	1.50	0.33	15	7.63	66
Tank A	0.81	0.29	24	12.51	60
D32H18	0.56	0.16	37	4.6	50
D08H06	0.75	0.32	31	19.1	50

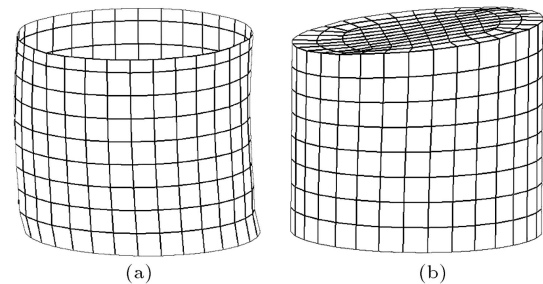


Figure 9. Typical mode shapes: (a) Impulsive; and (b) convective.

and m_{01} are frequency and mass participation of sloshing and impulsive modes, respectively. The typical dominant mode shapes of the tanks are shown in Figure 9.

4.3. Time history analysis

For each tank, ten time history analyses have been performed, seven of the analyses were related to seven real earthquake records. Then 3 time history analyses were performed by using 3 “ETA20e” series acceleration functions. Finally, the average results of 7 earthquake record analyses were compared with an average result of 3 acceleration functions. In Table 4, the specifications of 7 earthquake records related to series “ETA20e” of ET method are shown. Scale factors are used to match their intensity with code requirements [14].

The following graphs are related to solid shell and sloshing fluid of Tank A under record no. 1. The frequency of shell parameters is high showing rapid converge to stable state, but the frequency of fluid parameters is low with slow converge to stable state. The interface of impulsive and convective modes accompanied by small oscillation on long waves can be noticed. Displacement of solid shell is on a horizontal plane and displacement of fluid (wave height) is vertical to the surface. In Figure 10, the shell displacement graph of node 1 in seismic direction is presented, as it had been shown in Figure 7(c).

In Figure 11, the fluid displacement time history graph of node 2 is presented, as it was shown earlier in

Table 4. Specification of selected earthquake records.

Records no.	Record name	Earthquake name	Year	Magnitude (richter scale)	Duration (sec)	Time sampling (sec)	Scale factor
1	LADSP000	Landers	1992	7.5	50.0	0.020	3.64
2	LPAND270	Loma Prieta	1989	7.1	39.6	0.005	2.61
3	LPGIL067	Loma Prieta	1989	7.1	39.9	0.005	2.21
4	LPLOB000	Loma Prieta	1989	7.1	39.9	0.005	2.29
5	LPSTG000	Loma Prieta	1989	7.1	39.9	0.005	1.44
6	MHG06090	Morgan Hill	1984	6.1	29.9	0.005	1.84
7	NRORR360	Northridge	1994	6.8	40.0	0.020	1.07

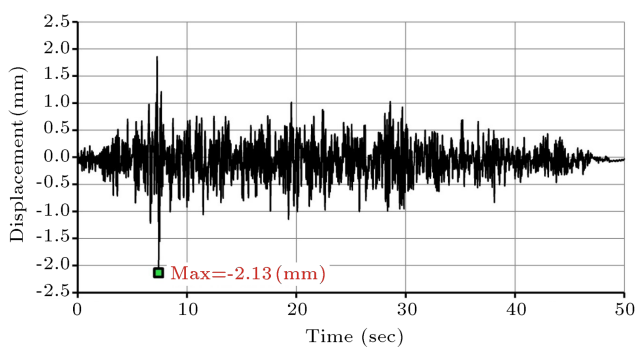
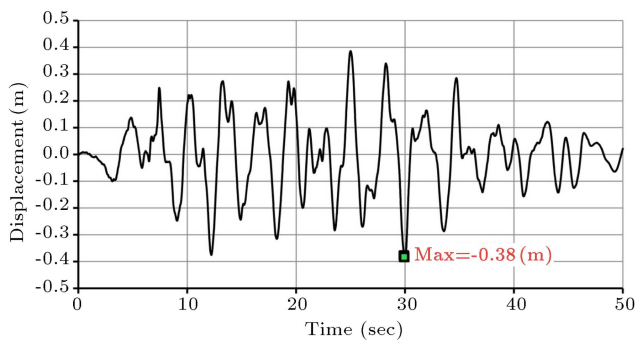
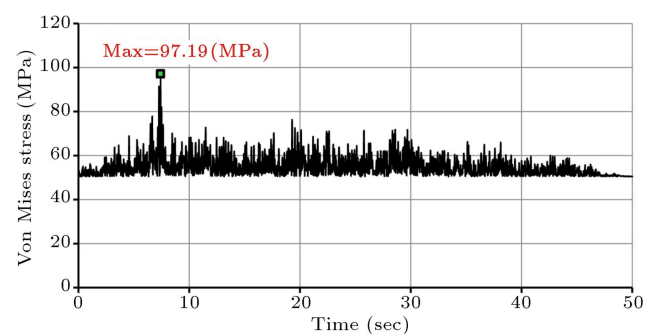
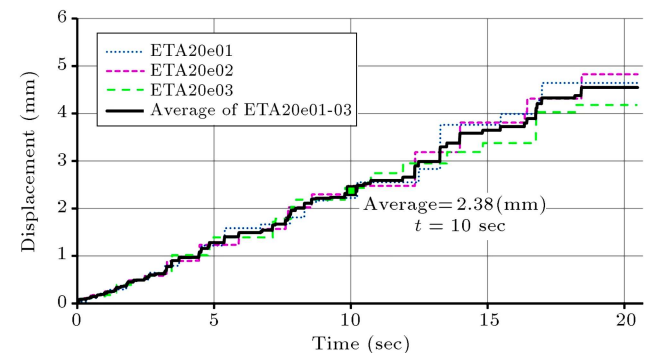
**Figure 10.** Shell displacement time history of node 1 in seismic direction.**Figure 11.** Fluid displacement time history of node 2.

Figure 7(c). Comparison of Figures 10 and 11 shows that the displacement levels and the oscillation period of fluid are higher than that of the shell wall. In addition, it is observed that fluid fluctuations take time in order to reach a stable state as compared to the shell itself.

In Figure 12, the maximum von Mises stress time history graph is shown. In this graph, minimum stress value is 50.4 MPa, which is a result of hydrostatic pressure. After applying earthquake record to the tank, stress at the highest point is raised to 97.2 MPa.

Some seismic results, such as base shear, overturning moment and maximum von Mises stress for Tank A are shown in Table 5. Also, the average results of all tanks are summarized in Table 6.

**Figure 12.** Maximum von Mises stress time history response.**Figure 13.** Shell displacement time history of node 1 in seismic direction.

4.4. Endurance time analysis

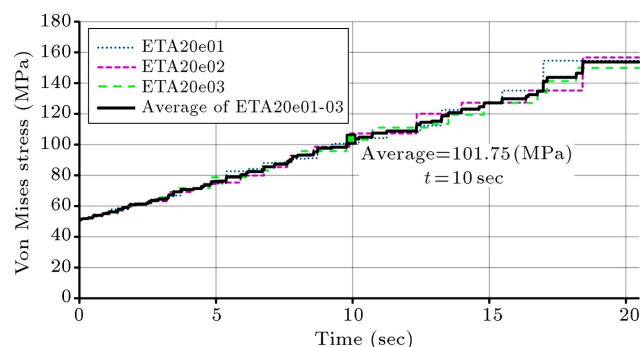
“ETA20e” series includes 3 acceleration functions. The “ETA20e” series is based on the average response spectrum of ground motions and is applicable to nonlinear analyses [4]. The duration of these acceleration functions is 20.48 seconds with sampling time of 0.01 second. If we draw ET curves [6,7] and observe the results on the target time of the tenth second, the effective excitation from ET will be equivalent of those from scaled ground motions. It is possible to compare the results of ET with the results of TH (earthquake time history) analyses. In Figure 13, the shell displacement ET curve of node 1 (see Figure 7(c)), is presented.

Table 5. Summary of response quantities for Tank A.

Record no.	Base shear (MN)	Overturning moment (MNm)	Maximum von Mises stress (MPa)	Maximum shear stress (MPa)	Maximum displacement of shell (mm)	Maximum wave height (mm)
1	4.43	15.89	97.2	53.8	2.60	396
2	3.25	11.78	85.0	46.9	2.40	508
3	5.63	19.63	107.0	60.0	3.60	360
4	5.24	17.89	108.7	60.4	3.60	176
5	3.65	11.33	89.1	49.1	2.30	614
6	3.10	9.94	83.7	45.9	2.10	353
7	2.55	9.48	78.0	42.6	2.00	382
Average	3.98	13.71	92.7	51.3	2.66	398

Table 6. Summary of analysis results of all tanks.

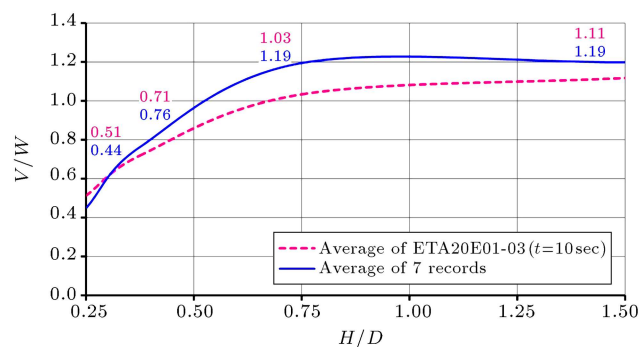
Tank name	Base shear (MN)	Overturning moment (MNm)	Maximum von Mises stress (MPa)	Maximum shear stress (MPa)	Maximum displacement of shell (mm)	Maximum wave height (mm)
D48H12	84.8	474	269	149	30.3	446
D32H12	64.0	307	317	167	30.8	567
D16H12	25.1	124	276	151	17.3	426
D08H12	6.4	35.2	198	114	11.7	627
Tank A	4.0	13.7	92.7	51.3	2.66	398
D32H18	128.6	946	293	159	35.9	606
D08H06	1.3	2.67	59.2	31.9	1.30	624

**Figure 14.** ET maximum von Mises stress time history response.

In Figure 14, the maximum von Mises stress ET curve for Tank A is shown. In this graph, average minimum stress value is 50.44 MPa, which is a result of hydrostatic pressure. After applying ET accelerograms to the tank at the highest point, average stress is raised to 101.75 MPa.

In Table 7, ET analyses results of some parameters for Tank A are depicted, and the average ET results in all tanks are also shown in Table 8.

In four of the seven tanks in which the height of the shell and the level of fluid are the same, the maximum of the normalized base shear, normalized

**Figure 15.** Base shear over weight (V/W) against H/D .

overturning moment, von Mises stress, shear stress and shell displacement figures have been plotted (Figures 15-19).

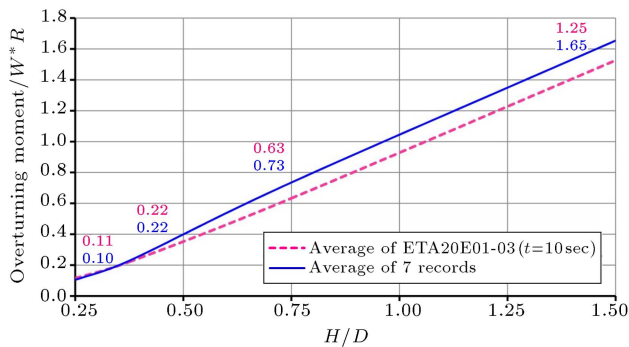
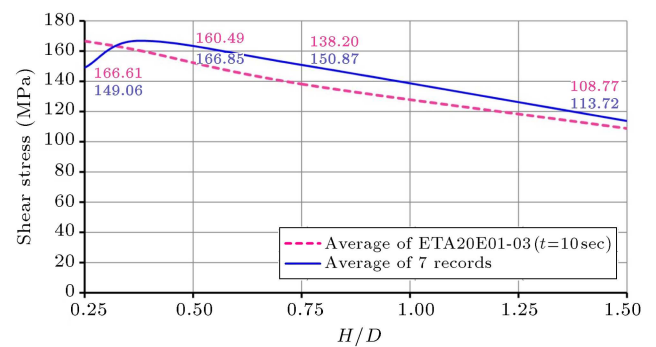
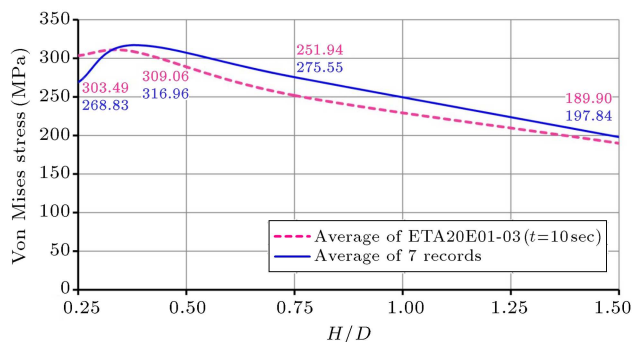
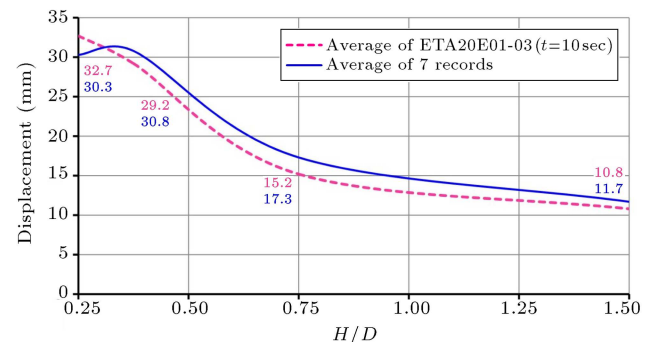
In Figures 15 and 16 there is an ascending slope between the normalized base shear and the normalized overturning moment with H/D , which shows these parameters have a direct relationship with the height to diameter of the tanks. Base shear (V) has been normalized to the total weight (W) of each tank and the overturning moment has been normalized to the product of total weight (W) of each tank multiplied by its radius (R). In Figures 15 and 16, a comparison of the normalized base shear and the normalized over-

Table 7. Linear results at $t = 10$ of Tank A subjected to “ETA20e” series.

Function name	Base shear (MN)	Overturning moment (MNm)	Maximum von Mises stress (MPa)	Maximum shear stress (MPa)	Maximum displacement of shell (mm)	Maximum wave height (mm)
ETA20e01	5.00	17.7	103	57.2	3.10	433
ETA20e02	4.82	16.5	102	56.5	3.10	417
ETA20e03	4.78	16.4	101	56.1	3.20	490
Average	4.87	16.9	102	56.6	3.13	447

Table 8. Averages linear results at $t = 10$ of all tanks subjected to “ETA20e” series.

Tank name	Base shear (MN)	Overturning moment (MNm)	Maximum von Mises stress (MPa)	Maximum shear stress (MPa)	Maximum displacement of shell (mm)	Maximum wave height (mm)
D48H12	97.0	521	303	167	32.7	390
D32H12	60.3	297	309	160	29.2	549
D16H12	21.7	107	252	138	15.2	469
D08H12	5.95	32.5	190	109	10.8	529
Tank A	4.87	16.9	102	56.6	3.13	447
D32H18	148	1126	322	174	40.7	624
D08H06	1.40	3.18	61.3	33.1	1.30	511

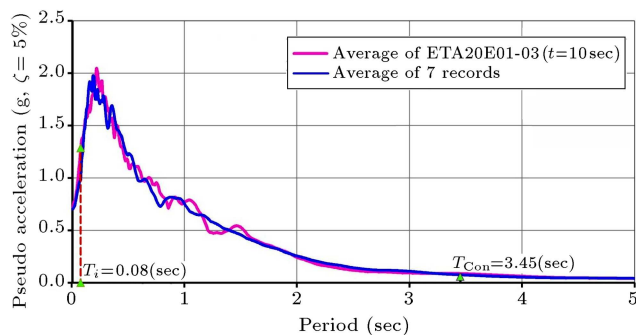
**Figure 16.** Overturning moment / ($W \cdot R$) against H/D .**Figure 18.** Shear stress against H/D .**Figure 17.** Von Mises stress against H/D .**Figure 19.** Shell displacement against H/D .

turning moment between the ground motion ensemble and ET analyses are presented. While the normalized base shear remains relatively constant for H/D higher than about 0.7, the overturning moment shows a linear increasing trend as expected.

In Figure 17, the von Mises stress according to ground motion and ET analyses are compared. In Figures 17-19, a similar trend between ground motion and ET analyses is observed, except for the tank having $H/D = 0.25$ in which there is a descending slope

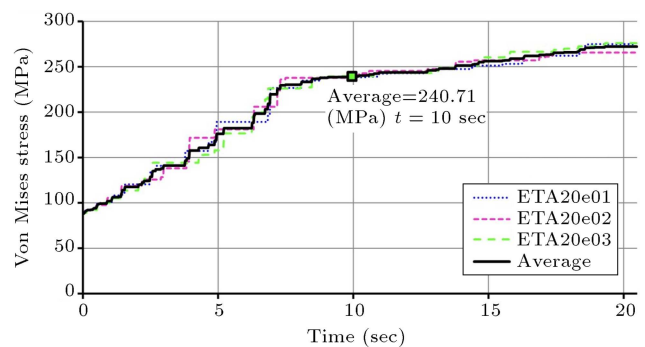
Table 9. Percentage difference between TH and ET results.

Tank name	Base shear	Overturning moment	Maximum von Mises stress	Maximum shear stress	Maximum displacement of shell	Maximum wave height
D48H12	14%	10%	13%	12%	8%	-13%
D32H12	-6%	-3%	-2%	-4%	-5%	-3%
D16H12	-13%	-14%	-9%	-8%	-12%	10%
D08H12	-7%	-8%	-4%	-4%	-7%	-16%
Tank A	22%	23%	10%	10%	18%	12%
D32H18	15%	19%	10%	9%	13%	3%
D08H06	9%	19%	4%	4%	3%	-18%

**Figure 20.** Dominant periods of tank.

between stress and H/D and between displacement and H/D . Figure 18 shows a comparison of shear stress according to ground motion and ET analyses. Comparison of shell displacement between ET analyses and ground motion analyses are shown in Figure 19, and in Figure 20 the average response spectra of “ET” acceleration functions and earthquake records are shown.

Here, the crossing points of two dominant periods with two response spectra are shown. It is clear that at the impulsive period, ET average response spectrum is above the average earthquake response spectrum. Based on this observation, after analysis, it is found that some parameters that depend on the impulsive period have greater quantity in ET than earthquake records. According to this fact, the percentage difference between TH and ET is positive. In Tank D32H12 at the impulsive period, ET’s average response spectrum is lower than the average response spectrum of the earthquake records. For example, the base shear in ET for this tank is less than the base shear for earthquake records, while the percentage difference between TH and ET is negative. In Table 9, the difference percentage between responses in earthquake time history and ET analyses are calculated. Also it may be observed here that the dimensions and the level of fluid of the tanks have affected the percentage differences between results of TH and ET.

**Figure 21.** ET maximum von Mises stress time history nonlinear response in Tank D32H12.

4.5. Nonlinear analysis

Three tanks were analyzed assuming nonlinear material behavior. Based on the limitations of the FE software, when fluid elements were included in the model, large deflections could not be calculated, and in effect, geometric nonlinearity could not be considered. Accordingly, in Tank A we ignored fluid elements and added fluid mass to the shell, similar to the add-mass procedure proposed by Barton and Parker [15]. This helps considering both nonlinearities (geometric and material nonlinearity) in this tank, but in the remaining two tanks (D32H12 and D32H18) we had fluid elements and only material nonlinearity was considered. In general, material nonlinearity has little effects on the overall seismic responses of the tanks because these tanks have been designed according to codes that are based on elastic design. However, some local yielding could be noticed near the base, where ET curves show the nonlinear effect. According to the bilinear kinematic stress-strain model, the increase in stress above the yield line depends on the ascending slope on the plastic region of stress-strain model. In effect, after a particular intensity level, yielding results in a reduced slope, as it occurs at about 8 sec, shown in Figure 21.

In Table 10, earthquake average nonlinear responses for the 3 tanks are presented, and the average ET nonlinear responses in these tanks are also shown

Table 10. Averages nonlinear results of three tanks subjected to earthquakes.

Tank name	Base shear (MN)	Overturning moment (MNm)	Maximum von Mises stress (MPa)	Maximum shear stress (MPa)	Maximum displacement of shell (mm)	Maximum wave height (mm)
Tank A	5.68	49.1	126	65.0	2.50	-
D32H12	56.0	278	233	120	45.0	564
D32H18	120	939	227	122	49.1	602

Table 11. Averages nonlinear results at $t = 10$ of three tanks subjected to "ETA20e" series.

Tank name	Base shear (MN)	Overturning moment (MNm)	Maximum von Mises stress (MPa)	Maximum shear stress (MPa)	Maximum displacement of shell (mm)	Maximum wave height (mm)
Tank A	5.99	53.5	123	63.8	3.00	-
D32H12	57.6	287	240	123	38.8	511
D32H18	140	1058	241	129	52.8	589

Table 12. Percentage difference between TH and ET results.

Tank name	Base shear	Overturning moment	Maximum von Mises stress	Maximum shear stress	Maximum displacement of shell	Maximum wave height
Tank A	6%	9%	-2%	-2%	19%	-
D32H12	3%	3%	3%	3%	-14%	-10%
D32H18	17%	13%	6%	6%	7%	-2%

in Table 11. Though nonlinear shell material for Tanks D32H12 and D32H18 has been used, the results obtained are close to linear results. But for Tank A with both nonlinearities (geometric and material nonlinearity), the results have a greater difference in comparison to linear results.

In Table 12, the difference percentage between responses in earthquake time history and ET analyses are calculated for nonlinear results. This shows the reliability of the ET method in predicting the response of models considering nonlinear material and geometric nonlinearity.

5. Summary and conclusions

In this paper, linear and nonlinear seismic responses of steel tanks underground motions and ET excitation functions have been compared. Linear and nonlinear time history analyses have been performed to obtain the structure and fluid responses. All of the tanks are cylindrical, they are supported and anchored on a rigid ground base. The following conclusions can be drawn:

1. The comparison between the results of ground motions and ET acceleration functions implies that

results are generally compatible and endurance time method can be used in order to estimate the average response of anchored tanks to ground motions in almost all practically relevant height to diameter ratios.

2. The percentage difference between the results of the three acceleration functions is quite small; therefore, a single response history analysis using only one of these ET acceleration functions can be considered instead of the average of three analyses when a rough estimate is adequate.
3. Some of the responses, such as wave height, depend on the sloshing period while some other responses, such as reaction force, depend on impulsive period. This fact can be considered so that a better estimation of response can be worked out considering appropriate intensity measures.
4. Existence of fluid elements along with other specific elements, heavily increases the computational demand required for a realistic analysis. By using the endurance time method, the required computational demand, especially when multilevel response analysis is required, can be considerably reduced. This can be beneficial when an approximate esti-

mation is acceptable, such as in design optimization requiring a relatively large number of trial and error analyses.

Acknowledgments

The authors would like to acknowledge the support of Sharif University of Technology Research Council, and National Iranian Oil Engineering and Construction Co. (contract NIOEC2/ER-CV/CON-EX05-00) for supporting this research.

Nomenclature

$D_x H_y$	Tank with diameter x and height y
ET	Endurance Time
f_{01}	Frequency of impulsive part of tank (Hz)
f_1	Frequency of sloshing part of tank (Hz)
H	Depth of fluid in tank
H_c	Height of convective mass in analytic model
H_I	Height of impulsive mass in analytic model
H_r	Height of top of roof
H_t	Height of shell
H_t/D	Height to diameter
m_{01}	Mass participation percent of impulsive mode
m_1	Mass participation percent of sloshing mode
m_c	Convective or sloshing mass
M_c	Convective mass in analytic model
m_i	Impulsive mass
M_i	Impulsive mass in analytic model
P	Hydrostatic pressure
R	Radius of tanks
$S_{aC}(T)$	Code acceleration response for period T
$S_{aT}(T, t)$	Target acceleration response for period T at time t
T	Free vibration period
TH	Time History (especially for earthquake records)
t_n	Thickness of each course of shell plate from bottom to top $n = 1, 2, \dots, 6$
t_{Target}	Target time
γ	Specific gravity of fluid
W	Total weight of tank
V	Base shear

References

1. Housner, G.W. "Earthquake pressure on containers", California Institute of Technology, Project No. 081-095, Pasadena, California (1954).
2. Malhotra, P.K., Wenk, T. and Wieland, M. "Simple procedure for seismic analysis of liquid-storage tanks", *Structural Engineering and International*, **10**(3), pp. 197-201 (2000).
3. Zama, S., Nishi, H., Hatayama, K., Yamada, M., Yoshihara, H. and Ogawa, Y. "On damage of oil storage tanks due to the 2011 off the pacific coast of Tohoku earthquake (Mw9.0), Japan", *The Fifteenth World Conference on Earthquake Engineering*, Lisbon, Portugal (2012).
4. Estekanchi, H.E., Riahi, H.T. and Vafai, A. "Application of endurance time method in seismic assessment of steel frames", *Engineering Structures*, **33**(9), pp. 2535-2546 (2011).
5. Mirzaee, A. and Estekanchi, H. "Performance-based seismic retrofitting of steel frames by endurance time method", *Earthquake Spectra* (2013). doi: 10.1193/081312EQS262M
6. Vaezi, D. "Nonlinear seismic analysis of ground-supported steel storage tanks using endurance time method", MSc Thesis, Sharif University of Technology, Tehran (2008).
7. Vaezi, D., Estekanchi, H.E., Vafai, A. and Riahi, H.T. "Linear analysis of on ground oil reservoirs with endurance time method, using real earthquake compatible acceleration functions", (in Persian) *Sharif Journal of Science and Technology*, **26**(3), pp. 23-31 (2011).
8. Estekanchi, H.E. and Alembagheri, M. "Seismic analysis of steel liquid storage tanks by endurance time method", *Thin-Walled Structures*, **50**(1), pp. 14-23 (2012).
9. Hariri Ardebili, M., Mirzabozorg, H. and Kianoush, R. "A study on nonlinear behavior and seismic damage assessment of concrete arch dam-reservoir-foundation system using endurance time analysis", *International Journal of Optimization in Civil Engineering*, **2**(4), pp. 573-606 (2012).
10. Alembagheri, M. and Estekanchi, H.E. "Seismic assessment of unanchored steel storage tanks by endurance time method", *Earthquake Engineering and Engineering Vibration*, **10**(4), pp. 591-604 (2011).
11. Endurance Time Method Website, 2013, <https://sites.google.com/site/etmethod/>
12. Valamanesh, V. and Estekanchi, H.E. "Endurance time method for multi-component analysis of steel elastic moment frames", *Scientia Iranica*, **18**(2), pp. 139-142 (2011).
13. API-650, "Welded steel tanks for oil storage", *API Standard 650*, American Petroleum Institute, Washington, D.C. (2005).

14. “Iranian seismic design code for oil industries”, Engineering Deputy of Iran Ministry of Oil (2007).
15. Barton, D.C. and Parker, J.V. “Finite element analysis of the seismic response of anchored and unanchored liquid storage tanks”, *Earthquake Engineering & Structural Dynamics*, **15**(3), pp. 299-322 (1987).

Biographies

Danial Vaezi has a Master of Science in Structural Engineering from Sharif University and a BSc in Civil Engineering from the College of Engineering at the University of Tehran. He has experience in designing structures and has worked on seismic analysis of steel oil tanks.

Homayoon Estekanchi is a professor of Civil Engineering at Sharif University of Technology. He received his PhD in Civil Engineering from SUT in

1997 and has been a faculty member at SUT since then. He is a member of Iranian Construction Engineers Organization, ASCE, Iranian Inventors Association and several other professional associations. His research interests include a broad area of topics in structural and earthquake engineering with a special focus on the design of tall buildings and industrial structures.

Abolhassan Vafai is a Professor of Civil Engineering at Sharif University of Technology. He has authored/co-authored numerous papers in different fields of Engineering: Applied Mechanics, Biomechanics, Structural Engineering (steel, concrete, timber and offshore structures). He has also been active in the area of higher education and has delivered lectures and published papers on challenges of higher education, the future of science and technology and human resources development.